ARTICLE NO. 78-382

Entrainment Limits in Heat Pipes

C.L. Tien* and K.S. Chung†
University of California, Berkeley, Calif.

The present work explores the physical basis for the entrainment limit in heat pipes and attempts to develop adequate quantitative criteria for the limit. Analogy is emphasized here between the entrainment phenomenon in heat pipes and the flooding phenomenon in countercurrent vapor-liquid flow systems. The maximum operating heat-transfer rates for various heat pipes due to entrainment limitation are established semiempirically by way of modifying existing flooding correlations. While the present results are successful in correlating the limited experimental data available, further experimental studies are needed in assessing the validity of the established criteria.

Introduction

As a device of very high thermal conductance, the heat pipe has nevertheless various operating limits to the maximum heat-transfer rate it can achieve. These limits, which include the boiling limit, the wicking limit, and various vapor flow limits such as the entrainment limit and the sonic limit, result from a breakdown or a rate limit in the circulation of the working fluid.[1-3] Considerable progress has been made in the study of these operating limits, but the entrainment limit has remained rather speculative and little understood. In contrast, an analogous phenomenon, the countercurrent flooding limit in vapor-liquid flow systems, has been investigated extensively in recent years.[4-6]

The entrainment or flooding limit has its origin in the interfacial interaction between the vapor and liquid flows. When the relative velocity between the vapor and liquid is sufficiently large, the interface becomes unstable and the destabilizing effects appear in the form of a wave at the interface. As the velocity increases, the enhanced wave action, together with the interfacial shear force, may become sufficient to overcome the liquid surface-tension force, and liquid droplets are thus formed from the surface and entrained into the vapor. The entrainment phenomenon is an early signal of an unstable flow condition that can develop into the highest level of the system instability by even a very small disturbance or perturbation. This thus leads to the partial or total stoppage of liquid flow or dryout. The phenomenon is generally characterized by the Weber number that compares the vapor inertial force to the liquid surface-tension force.

In heat pipes, the entrainment phenomenon becomes much more complicated, due to the presence of the capillary structure. Cotter[7] first applied the hydrodynamic instability concept to horizontal wicked heat pipes and Kemme[3] later included the gravity effect for the vertical gravity-assisted operation. Their criteria are expressed in terms of the Weber number containing a characteristic wavelength. Interpretation of this characteristic wavelength, which should be a function of capillary structures and flow properties, constitutes the critical element of the problem. Kemme[3] used the diameter of wires plus the wire gap to represent the characteristic wavelength for wicked heat pipes, while Feldman,[8] following the argument of Tippets,[9] assumed a surface wavelength approximately proportional to the liquid film thickness for grooved heat pipes. Experimental information is relatively scarce to render a conclusive assessment of the entrainment limit.

The present paper reports an attempt to develop adequate quantitative criteria for the entrainment limit in heat pipes. Instead of directly interpreting the Weber number criterion, emphasis here is placed on the use and extension of the existing flooding correlations in countercurrent vapor-liquid flow systems. These correlations, while semiempirical in nature, are relatively well established experimentally. On this basis, the entrainment limits for various heat pipes have been developed and the calculated maximum heat-transfer rates correlate favorably with the limited experimental data available. The present study points to the need for further analytical and experimental studies of the entrainment limit in heat pipes.

Countercurrent Flooding Correlations

There exist many forms of empirical flooding correlations for countercurrent vapor-liquid flow systems due to its wide applications in chemical, mechanical, and nuclear industries. The most commonly used flooding correlation has been the Wallis correlation which characterizes a balance of inertial forces and hydrostatic forces:

$$(j_g^*)^{1/2} + (j_f^*)^{1/2} = c_w \tag{1}$$

where $c_w \approx 0.7\text{-}1.0$, both constants determined empirically from experiments. The dimensionless momentum fluxes of gas and liquid are defined by:

$$j_g^* = \left[\frac{\rho_g j_g^2}{gL(\rho_f - \rho_g)}\right]^{1/2} \qquad j_f^* = \left[\frac{\rho_f j_f^2}{gL(\rho_f - \rho_g)}\right]^{1/2} \tag{2}$$

where ρ is density, j is velocity, g is gravitational acceleration, and subscripts f and g refer to liquid and gas, respectively. The characteristic length L is commonly identified to the hydraulic diameter D of the flow passage.[5]

Another flooding correlation[10] that has met increasing popularity is expressed in terms of the Kutateladze dimensionless groups[6]

$$(K_g)^{1/2} + (K_f)^{1/2} = c_k \tag{3}$$

where $c_k = \sqrt{3.2}$ and

$$K_g = \frac{\rho_g^{1/2} j_g}{[g\sigma(\rho_f - \rho_g)]^{1/4}} \qquad K_f = \frac{\rho_f^{1/2} j_f}{[g\sigma(\rho_f - \rho_g)]^{1/4}} \tag{4}$$

Presented as Paper 78-382 at the 3rd International Heat Pipe Conference, Palo Alto, Calif., May 22-24, 1978; submitted June 20, 1978; revision received Feb. 9, 1979. Copyright © American Institute of Aeronautics and Astronautics, Inc., 1978. All rights reserved.

Index categories: Heat Pipes; Thermal Control; Multiphase Flows.

*Professor, Dept. of Mechanical Engineering, Associate Fellow AIAA.

†Graduate Research Assistant, Dept. of Mechanical Engineering; presently with the Argonne National Laboratory, Argonne, Ill.

with σ as surface tension. The dimensionless group K signified a balance of dynamic head, surface tension, and gravity force.

Comparing Eqs. (1) and (3) indicates that they are identical if the characteristic length L is identified as:

$$L=\left(\frac{c_k}{c_w}\right)^4\left[\frac{\sigma}{g(\rho_f-\rho_g)}\right]^{1/2} \tag{5}$$

which is indeed the critical wavelength of Taylor instability:

$$\lambda_t=c_t\left[\frac{\sigma}{g(\rho_f-\rho_g)}\right]^{1/2} \quad (2\pi<c_t<2\pi\sqrt{3}) \tag{6}$$

It is also interesting to note that λ_t plays a significant role in the successful prediction of maximum heat flux in pool boiling based on a model of countercurrent flooding.[11] Equations (5) and (6) strongly suggest the role of wave instability in the flooding or entrainment phenomenon.

The diameter of the vapor flow passage, which is absent in Eq. (3), does affect the flooding characteristics. Extensive experimental data[12-14] for the limiting case of total flooding ($j_f=0$) show that the applicability of Eq. (1) with $L=D$ and Eq. (3) depends on the magnitude of the Bond number, a dimensionless tube diameter defined by:

$$Bo=D[g(\rho_f-\rho_g)/\sigma]^{1/2} \tag{7}$$

For large Bo (say, greater than 30), Eq. (3) correlates data successfully and demonstrates no dependence on D, while Eq. (1) with $L=D$ applies well for small Bo (say, less than 10). For convenience of correlations, the following expression is suggested for application in the entire range of Bo:

$$(K_g)^{1/2}+(K_f)^{1/2}=\sqrt{3.2}\tanh(0.5Bo^{1/4})\equiv C_K \tag{8}$$

which becomes Eq. (3) when $Bo \gg 1$ and approaches to Eq. (1) for small Bo as shown in Fig. 1. Equation (8) will be used as the basis in formulating the entrainment limit in various heat pipes.

Entrainment Limits for Various Heat Pipes

Gravity-Assisted Wickless Heat Pipes

Since the flooding correlations just discussed still contain certain uncertainties, especially in the constants of c_w and c_k which depend on the flow entry conditions,[5-14] it is important to assess the validity of these correlations in their applications to the heat pipe without first getting into the complexities of the capillary structure. The gravity-assisted wickless heat pipe or thermosyphon is the perfect candidate for such an assessment, as the flooding condition inside is nearly identical to the conventional countercurrent case except for the difference in flow entries. Experimental data are also available for a variety of operating conditions, working fluids, and pipe sizes.[15-18]

The maximum heat-transfer rate due to entrainment limitation can be calculated through the flooding correlations in conjunction with the following relations based on the mass and energy balance under the steady-state operation of a heat pipe:

$$Q/A_x=\rho_f j_f h_{fg}=\rho_g j_g h_{fg} \tag{9}$$

where A_x is the cross-sectional area of the heat pipe flow passage. Substituting j_f and j_g of Eq. (9) into Eq. (8) gives:

$$Q=C_K^2 A_x h_{fg}[\rho_f^{-1/4}+\rho_g^{-1/4}]^{-2}[g\sigma(\rho_f-\rho_g)]^{1/4} \tag{10}$$

It is interesting to note that Eq. (10) is of the same form as that established for the maximum heat-transfer rate in pool boiling based on a flooding model.[11]

Comparison with experimental data is shown in Fig. 2, where Q_K in the dimensionless maximum heat flux Q/Q_K refers to the predicted maximum heat flux given by Eq. (10). Considering the very different operating conditions, working fluids, and pipe sizes, the experimental data agree remarkably well with Eq. (10) (i.e., $Q/Q_K=1$). The only large deviation comes from the one point of Frea[16] which has a very small value of the Bond number and is outside of the correlation range as pointed out previously.[13] Also plotted on Fig. 2 are the Wallis correlations with $c_w=0.7$ and 1.0, and the curve with $c_w=0.7$ correlates well with the data.

Gravity-Assisted Wicked Heat Pipes

The gravity-assisted wicked heat pipe has become increasingly popular in terrestrial applications because of its high heat-transfer performance and less stringent requirement on the wick structure. In calculating the entrainment-limited maximum heat-transfer rate for the gravity-assisted wicked heat pipe, however, the ordinary flooding correlation must be

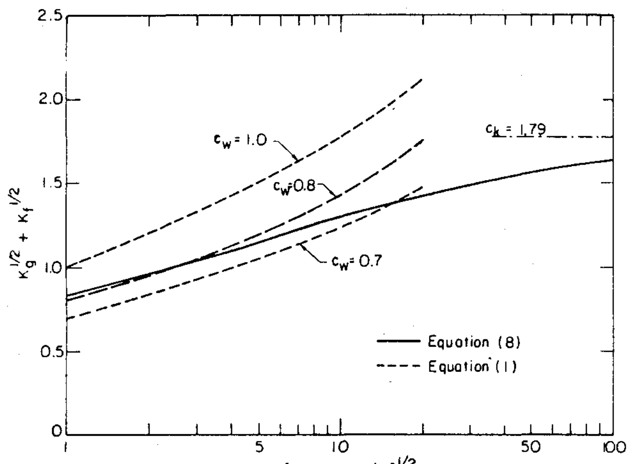

Fig. 1 Comparison of flooding correlations.

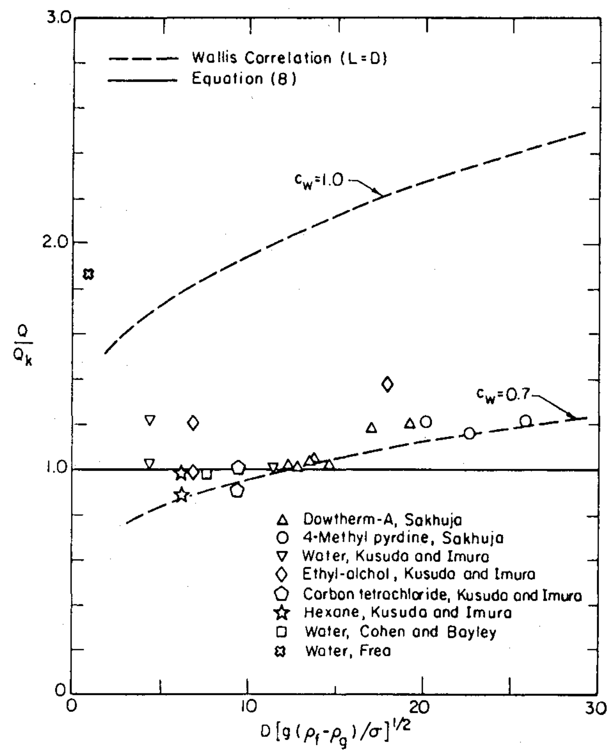

Fig. 2 Maximum heat-transfer rate in gravity-assisted wickless heat pipes.

modified to take into account the effect of capillary structure. The logical step would be to modify the critical wavelength as given in Eq. (6). Since the critical wavelength depends on the characteristic length h of the capillary structure (e.g., opening of the screen wick) and λ is proportional to h, the simplest modification would be:

$$\lambda = c_t\left(\frac{h}{D}\right)\left[\frac{\sigma}{g(\rho_f-\rho_g)}\right]^{1/2} \tag{11}$$

where the characteristic length D of the heat pipe (e.g., pipe diameter) is placed in the denominator on the basis of dimensional consideration. The added factor (h/D) can also be rationalized by the following argument: For wickless heat pipes, $\lambda_t/2 \sim$ wave amplitude $\sim D/2$, while $\lambda \sim h$ for wicked heat pipes; thus, $(\lambda/\lambda_t) \sim (h/D)$. It should be realized that Eq. (11) applies in the range $(h/\lambda_t) \lesssim 1$, since Eq. (6) is valid for $(h/\lambda_t) \gg 1$ or $h \gg \lambda_t$.

Substituting λ given in Eq. (11) for L in Eqs. (1) and (2) gives the following flooding correlation:

$$(K_g)^{1/2} + (K_f)^{1/2} = C_K (D/h)^{1/4} \tag{12}$$

Accordingly, the maximum heat-transfer rate for the gravity-assisted wicked heat pipe can be obtained from Eqs. (9) and (12) as:

$$Q = C_K^2 (D/h)^{1/2} A_x h_{fg} [\rho_f^{-1/4} + \rho_g^{-1/4}]^{-2} [g\sigma(\rho_f - \rho_g)]^{1/4} \tag{13}$$

As shown in Fig. 3, the experimental results reported by Kemme[3] for a long, gravity-assisted sodium heat pipe are in good agreement with Eq. (13), where h is taken as 1.59 mm corresponding to the wire diameter, plus the distance between wires of the 16-mesh screen. The same value of h has been used by Kemme in his correlation[3] which has an expression similar to Eq. (13), but which was obtained by simply adding an additional balancing force term of buoyancy to the Weber number criterion as suggested by Cotter.[1] Also shown in Fig. 3 are the data obtained from a different gravity-assisted sodium heat pipe,[19] which exhibit several maximum heat-transfer limits in different temperature ranges. The calculated entrainment limit agrees well with the experimental data, although some empiricism is introduced here by arbitrarily using the value of h corresponding to the 34-mesh screen due to the lack of definitive wick-structure information.

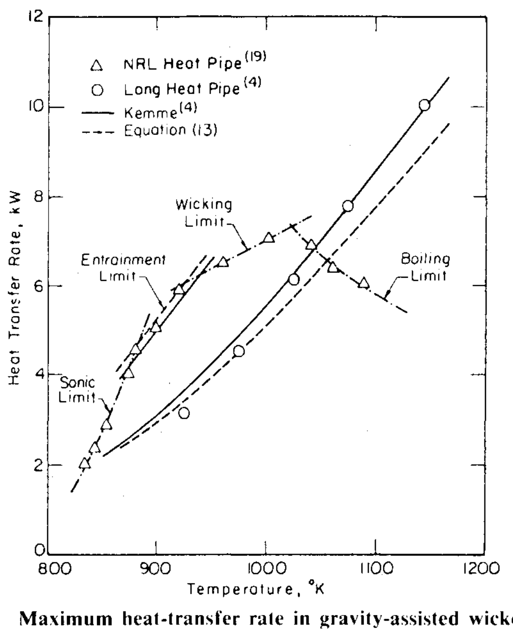

Fig. 3 Maximum heat-transfer rate in gravity-assisted wicked heat pipes.

Horizontal Wicked Heat Pipes

There has been doubt concerning the existence of the entrainment limit in horizontal wicked heat pipes.[20] Experimentally, it is difficult to identify conclusively whether the dryout limit is due to entrainment or other physical mechanisms. The analytical argument[20] as advanced, however, is based on the conventional Weber number criterion, the direct application of which to wicked systems is also subject to question. Despite these uncertainties, it would be of interest to establish the entrainment limit of horizontal wicked heat pipes according to the present approach and to compare with measurements.

Recognizing the absence of gravity (neglecting the azimuthal-direction effect), and the presence of capillary structure characterized by h, the flooding correlation assumes the following form from simple dimensional consideration:

$$\left[\frac{j_g \rho_g^{1/2}}{(\sigma/h)^{1/2}}\right]^{1/2} + \left[\frac{j_f \rho_f^{1/2}}{(\sigma/h)^{1/2}}\right]^{1/2} = C_K \tag{14}$$

The corresponding maximum heat-transfer rate is given by:

$$Q = C_K^2 A_x h_{fg} \left(\frac{\sigma}{h}\right)^{1/2} [\rho_f^{-1/4} + \rho_g^{-1/4}]^{-2} \tag{15}$$

The comparison between Eq. (15) and experimental data is shown in Fig. 4, along with the calculated curves suggested by Kemme, who termed the limiting phenomenon as the vapor pressure drop limitation. Without much arbitrary adjustment of h (equivalent mesh of 120 used in test 4 due to the non-square opening of 200×115 mesh), Eq. (15) correlated remarkably well with the experimental data.

Grooved Heat Pipes

For grooved heat pipes, the characteristic length h of the capillary structure is best characterized by the groove width.[21] Other than the ordinary flooding correlation constant c_k that may assume a slightly different value from $\sqrt{3.2}$, the same entrainment-limit correlations for wicked heat pipes should be applicable: Eqs. (12) and (13) in the gravity-assisted cases and Eqs. (14) and (15) in the horizontal cases. The lack of pertinent experimental data, however, prevents verification of these correlations. A previous analysis[8] did arrive at a similar expression as suggested here for the horizontal cases.

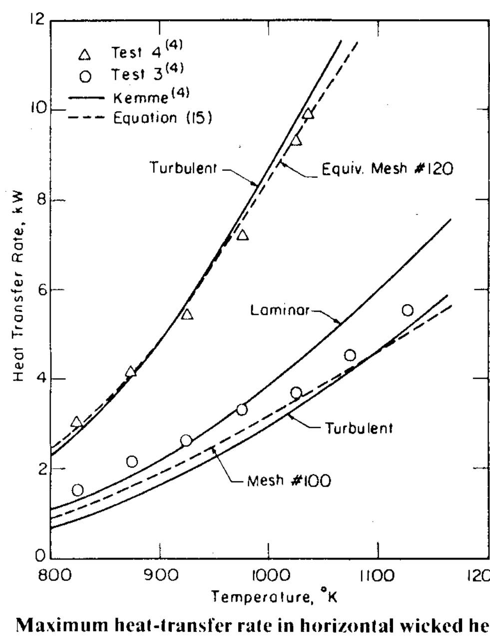

Fig. 4 Maximum heat-transfer rate in horizontal wicked heat pipes.

Rotating Heat Pipes

It is of interest to see how the present approach is applied to the case of rotating heat pipes that utilize the centrifugal force as the driving force.[22] Employing the same dimensional consideration, the entrainment-limit correlation for the rotating heat pipe can be established as:

$$\left[\frac{j_f \rho_f^{\,1/4}}{(\sigma D \omega^2 \sin\theta)^{1/4}}\right]^{1/2} + \left[\frac{j_g \rho_g^{\,1/4}}{(\sigma D \omega^2 \sin\theta)^{1/4}}\right]^{1/2} = C_K \qquad (16)$$

where D is the larger-side diameter, ω the angular frequency of rotation, and θ the tapering angle of the heat pipe. The corresponding maximum heat transfer is thus given by:

$$Q = C_K^2 A_x h_{fg} (\sigma D \omega^2 \sin\theta)^{1/4} (\rho_f^{-1/8} + \rho_g^{-1/8})^{-2} \qquad (17)$$

Again, the constant C_K might require some modification in this case. At present, no experimental data are available to verify the validity of Eqs. (16) and (17).

References

[1] Cotter, T.P., "Theory of Heat Pipes," Los Alamos Scientific Laboratory Rept. LA-3246-MS, 1965.

[2] Tien, C.L., "Fluid Mechanics of Heat Pipes," *Annual Review of Fluid Mechanics,* Vol. 7, 1975, pp. 167-185.

[3] Kemme, J.E., "Vapor Flow Considerations in Conventional and Gravity-Assist Heat Pipes," *Proceedings of 2nd International Heat Pipe Conference,* Vol. 1, 1976, pp. 11-22.

[4] Tien, C.L. and Liu, C.P., "A Survey on Vertical Two-Phase Counter-Current Flooding," Rept. NP-984, Electric Power Research Institute, Palo Alto, Calif., 1979.

[5] Wallis, G.B., *One Dimensional Two-Phase Flow,* McGraw-Hill Book Co., New York, 1969.

[6] Kutateladze, S.S., "Elements of Hydrodynamics of Gas-Liquid Systems," *Fluid Mechanics-Soviet Research,* Vol. 1, 1972, pp. 29-50.

[7] Cotter, T.P., "Heat Pipe Startup Dynamics," IEEE Conference Record of the Thermonic Conversion Specialist Conference, 1967, pp. 344-348.

[8] Feldman, K.T. and Thupvongsa, C., "Predicting Counter-Flow Shear Effects in Heat Pipes," AIAA Paper 77-749, 1976.

[9] Tippets, F.E., "Analysis of the Critical Heat Flux Condition in High Pressure Boiling Water Flows," *Journal of Heat Transfer,* Vol. 86, 1964, pp. 23-28.

[10] Tien, C.L., "A Simple Analytical Model for Counter-Current Flow Limiting Phenomena with Vapor Condensation," *Letters in Heat and Mass Transfer,* Vol. 4, 1977, pp. 231-238.

[11] Hsu, Y.Y. and Graham, R.W., *Transport Processes in Boiling and Two-Phase Systems,* McGraw-Hill Book Co., New York, 1976.

[12] Pushkina, O.L. and Sorokin, Yu. L., "Breakdown of Liquid Film Motion in Vertical Tubes," *Heat Transfer-Soviet Research,* Vol. 1, 1969, pp. 56-64.

[13] Wallis, G.B. and Makkencherry, S., "The Hanging Film Phenomenon in Vertical Annular Two-Phase Flow," *Journal of Fluids Engineering,* Vol. 96, 1974, pp. 297-298.

[14] Wallis, G.B. and Kuo, J.T., "The Behavior of Gas-Liquid Interfaces in Vertical Tubes," *International Journal of Multiphase Flow,* Vol. 2, 1976, pp. 521-536.

[15] Cohen, H. and Bayley, F.J., "Heat Transfer Problems of Liquid Cooled Gas Turbine Blades," *Proceedings of the Institute of Mechanical Engineers,* Vol. 169, 1955, pp. 1063-1074.

[16] Frea, W.J., "Two-Phase Heat Transfer and Flooding in Counter Current Flow," Paper B.5.10, *Proceedings of the 4th International Heat Transfer Conference,* Vol. 5, 1970.

[17] Kusuda, H. and Imura, H., "Boiling Heat Transfer in Open Thermosyphon," *Bulletin of Journal of the Society of Mechanical Engineers,* Vol. 16, 1973, pp. 1723-1733.

[18] Sakhuja, R.K., "Flooding Constraint in Wickless Heat Pipes," ASME Paper 73-WA/HT-7, 1973.

[19] Deverall, J.E., Keddy, E.S., Kemme, J.E., and Phillips, J.R., "Gravity-Assist Heat Pipes for Thermal Control Systems," Los Alamos Scientific Laboratory Rept. LA-5989-MS, 1975.

[20] Busse, C.A. and Kemme, J.E., "The Dry-Out Limits of Gravity-Assist Heat Pipes with Capillary Flow," AIAA Paper 78-383, 1978.

[21] Tien, C.L. and Sun, K.H., "Minimum Meniscus Radius of Heat Pipe Wicking Materials," *International Journal of Heat Mass Transfer,* Vol. 14, 1971, pp. 1853-1855.

[22] Gray, H.V., "The Rotating Heat Pipe—A Wickless, Hollow Shaft for Transferring High Heat Fluxes," ASME Paper 69-HT-19, 1969.